The EMBO Journal vol.14 no.1 pp.50–57, 1995

Co-localization of L-type Ca^{2+} channels and insulin-containing secretory granules and its significance for the initiation of exocytosis in mouse pancreatic B-cells

Krister Bokvist, Lena Eliasson, Carina Ämmälä, Erik Renström and Patrik Rorsman

Department of Medical Biophysics, Göteborg University, Medicinaregatan 11, S-413 90 Göteborg, Sweden

Communicated by B.Sakmann

We have monitored L-type Ca^{2+} channel activity, local cytoplasmic Ca^{2+} transients, the distribution of insulin-containing secretory granules and exocytosis in individual mouse pancreatic B-cells. Subsequent to the opening of the Ca^{2+} channels, exocytosis is initiated with a latency <100 ms. The entry of Ca^{2+} that precedes exocytosis is unevenly distributed over the cell and is concentrated to the region with the highest density of secretory granules. In this region, the cytoplasmic Ca^{2+} concentration is 5- to 10-fold higher than in the remainder of the cell reaching concentrations of several micromolar. Single-channel recordings confirm that the L-type Ca^{2+} channels are clustered in the part of the cell containing the secretory granules. This arrangement, which is obviously reminiscent of the 'active zones' in nerve terminals, can be envisaged as being favourable to the B-cell as it ensures that the Ca^{2+} transient is maximal and restricted to the part of the cell where it is required to rapidly initiate exocytosis whilst at the same time minimizing the expenditure of metabolic energy to subsequently restore the resting Ca^{2+} concentration.

Key words: Ca^{2+}/exocytosis/insulin/secretory granules

Introduction

It is well established that an elevation of the cytoplasmic Ca^{2+} concentration is essential for the initiation of insulin secretion from pancreatic B-cells, but the cellular and molecular processes involved have only partially been elucidated (Prentki and Matschinsky, 1987). Recent measurements from single B-cells, using capacitance measurements as an indicator of the exocytotic rate (Neher and Marty, 1982) have indicated that the exocytotic machinery operate at Ca^{2+} concentrations considerably higher than those actually measured using microfluorimetric techniques (Ämmälä *et al.*, 1993a). This suggests that the Ca^{2+} concentration in the vicinity of the plasma membrane may principally control the secretory machinery (Augustine and Neher, 1992). A problem inherent to measurements of localized cytoplasmic Ca^{2+} concentrations is that the ion has some, albeit low, mobility within the cytoplasm (Kasai and Petersen, 1994) and Ca^{2+} can be expected to equilibrate throughout the cytoplasm within 1 s. To date, most attempts to 'visualize' localized Ca^{2+} transients in the B-cell have been constrained by either insufficient temporal resolution and/or inability to control the membrane potential. One study, however, provided evidence that a single action potential evoked an increase in Ca^{2+} which was confined to one part of the B-cell (Theler *et al.*, 1992) but how this Ca^{2+} transient related to secretion was not determined. Here we have used a combination of the patch-clamp technique to record whole-cell or single-channel Ca^{2+} channel currents, capacitance measurements of exocytosis and digital imaging of cytoplasmic Ca^{2+} gradients and the distribution of secretory granules within the B-cell. This combination of techniques enabled us to demonstrate that the insulin-containing secretory granules and the voltage-dependent Ca^{2+} channel co-localize within the B-cell and that the Ca^{2+} transient need extend no more than ~1 μm from the plasma membrane to trigger exocytosis. This represents the first direct demonstration of such an organization, reminiscent of that in the nerve terminal, in a neuroendocrine cell.

Results

Localized depolarization-evoked Ca^{2+} transients

Figure 1A shows the secretory responses and average cytoplasmic calcium transients elicited by a series of depolarizations lasting 20–500 ms. Increasing the duration of the depolarization resulted in progressively larger $[Ca^{2+}]_i$ transients but steps shorter than 200 ms invariably failed to initiate exocytosis as revealed by the measurements of cell capacitance. By contrast, when similar experiments were performed without the Ca^{2+} indicator, a 50 ms depolarization was sufficient to evoke an exocytotic response (Figure 1B). The B-cell action potential lasts 50–100 ms (Atwater *et al.*, 1978). The observation that a depolarization as short as 50 ms elicits exocytosis in intact B-cells therefore suggests that single action potentials may be associated with insulin secretion *in vivo*. It is of interest that although $[Ca^{2+}]_i$ remains elevated for several seconds following a depolarization, exocytosis occurs during the stimulus only and stops immediately upon repolarization. This behaviour is easiest to explain by assuming that exocytosis is determined by the local $[Ca^{2+}]_i$ in the vicinity of the Ca^{2+} channels, which mirrors Ca^{2+} channel activity, and not by the average $[Ca^{2+}]_i$.

To determine the minimum distance over which Ca^{2+} needs to diffuse in order to elicit exocytosis, we next performed digital imaging of $[Ca^{2+}]_i$ during the 200 ms depolarization, i.e. the first depolarization that was associated with exocytosis. Figure 2A and B shows the whole-cell Ca^{2+} current elicited by the depolarization and images of the spatial distribution of $[Ca^{2+}]_i$ obtained at various times before, during and after the depolarization and activation of the Ca^{2+} channels. The increase in $[Ca^{2+}]_i$ was particularly pronounced in, and at short times

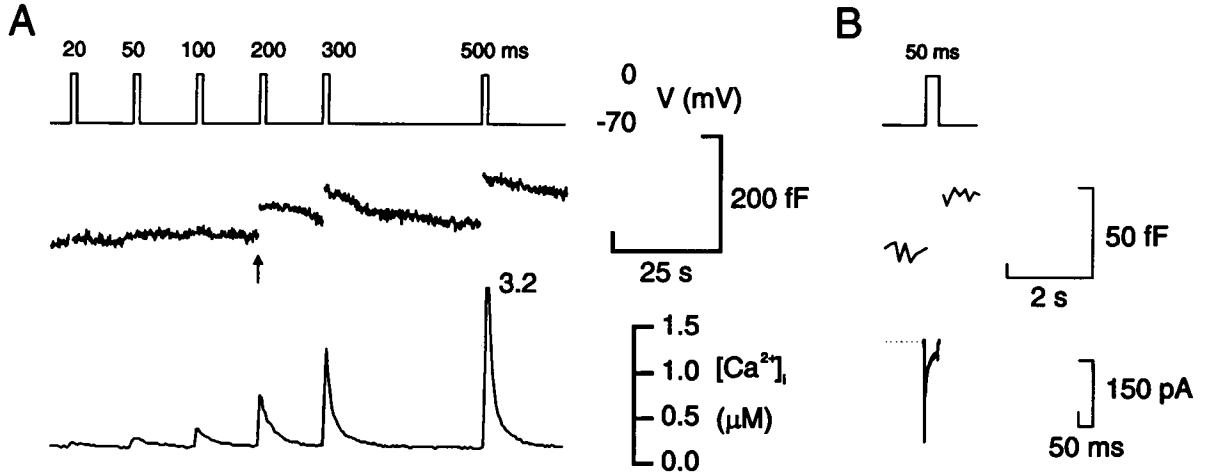

Fig. 1. Parallel recordings of Ca^{2+} transients and exocytosis in a single B-cell. (**A**) The duration of the voltage-clamp depolarizations from −70 to 0 mV was varied between 20 and 500 ms (top) and associated exocytotic responses (middle) and changes in average intracellular $[Ca^{2+}]_i$ (bottom). The resting $[Ca^{2+}]_i$ in this B-cell was 0.15 μM. The peak $[Ca^{2+}]_i$ during the 500 ms is truncated and reached a concentration of 3.2 μM. The arrow indicates the first exocytotic response (52 fF). (**B**) Exocytotic response to, and Ca^{2+} current evoked by, a 50 ms depolarization from −70 to 0 mV in an intact B-cell containing no extraneous Ca^{2+} buffers.

even confined to, the first 1–2 μm beneath the plasma membrane in the left part of the cell with the remainder being largely unaffected. This spatial heterogeneity becomes even clearer when the $[Ca^{2+}]_i$ profile of the cell is calculated (Figure 2C). At the end of the 200 ms depolarization, $[Ca^{2+}]_i$ reaches a concentration of 2.3 μM just beneath the membrane in the left part of the cell whilst remaining low (<0.5 μM) in the centre of the cell. The $[Ca^{2+}]_i$ gradients dissipate rapidly (within 300 ms) following repolarization and closure of the Ca^{2+} channels (Figure 2B, image e). Localized $[Ca^{2+}]_i$ increases such as those shown in Figure 2 were observed in >85% of the cells (n = 30; cf. Gylfe *et al.*, 1991; Theler *et al.*, 1992). The region of the cell in which the increase occurred varied between different cells. The increase occasionally took place in the vicinity of the patch electrode but equally often occurred in the opposite part of the cell and it is therefore unlikely that the spatial heterogeneity results from membrane deterioration due to the formation of the giga-seal. However, when the same cell was subjected to a train of depolarizations, the increase in $[Ca^{2+}]_i$ showed a large pulse-to-pulse reproducibility (data not shown).

Exocytosis was observed in only 30% of the cells loaded with the Ca^{2+} indicator (n = 9). In the six cells showing capacitance increases >20 fF (corresponding to the fusion of ~10 secretory granules using a conversion factor of 2 fF/granule; Ämmälä *et al.*, 1993a), the minimum average $[Ca^{2+}]_i$ required to induce exocytosis (65 ± 6 fF) was 2.5 ± 1.2 μM. Closer inspection of the data suggested the existence of steep spatial gradients of $[Ca^{2+}]_i$ within these B-cells. Thus, the 10% lowest and 10% highest fluorescence ratios corresponded to 0.6 ± 0.2 μM and 7.4 ± 4.3 μM, respectively.

Distribution of secretory granules and microfluorimetric detection of secretion

Earlier experiments have demonstrated that the fluorescent base quinacrine may be used to monitor exocytosis in secretory cells (Breckenridge and Almers, 1987) including the pancreatic B-cell (Pralong *et al.*, 1990). Available evidence suggests that in B-cells this dye is largely restricted to the secretory granules, where it can be envisaged to accumulate as a consequence of the interior of these organelles being slightly acidic (Abrahamsson and Gylfe, 1980), and degranulation of the B-cells is associated with the loss of quinacrine fluorescence (Lundquist *et al.*, 1985). Consequently, stimulation of insulin secretion can be monitored as an accelerated loss of quinacrine fluorescence. The data shown in Figure 3A indicate an uneven intracellular uptake of the dye and therefore imply that the secretory granules in this cell are concentrated in the upper left part of the cell. This reinforces previous ultrastructural experiments suggesting that the B-cell is polarized and that the secretory granules are restricted to the apical part of the cell (Bonner-Weir, 1988). An uneven distribution similar to that shown in Figure 3A was apparent in 50% of the cells investigated. In the remainder of the cells, the secretory granules formed a ring just beneath the plasma membrane.

Stimulation of secretion by application of depolarizing commands, with resulting activation of voltage-gated Ca^{2+} channels and stimulation of Ca^{2+} influx, produced both an increase in cell capacitance and a decrease in quinacrine fluorescence (Figure 3B). This observation was made in all investigated cells (n = 10). The decreased quinacrine fluorescence we attribute to the simultaneous release of insulin and quinacrine. This strongly suggests that a capacitance increase does indeed correspond to exocytosis of the insulin-containing secretory granules. It is of interest that quinacrine is not uniformly lost upon stimulation. For example, it appears that in Figure 3B, one pool of granules is capable of responding immediately upon stimulation (region i in Figure 3C) whereas a second pool (region ii in Figure 3C) requires more extensive stimulation before it is mobilized. Such regional differences were seen in 30% of the cells. It is possible that this is a consequence of the two pools being located at different distances from the point of Ca^{2+} entry.

Estimation of the number of secretory granules from the decrease in quinacrine fluorescence

By correlating the loss of quinacrine fluorescence to the concomitant change in cell capacitance it is possible to

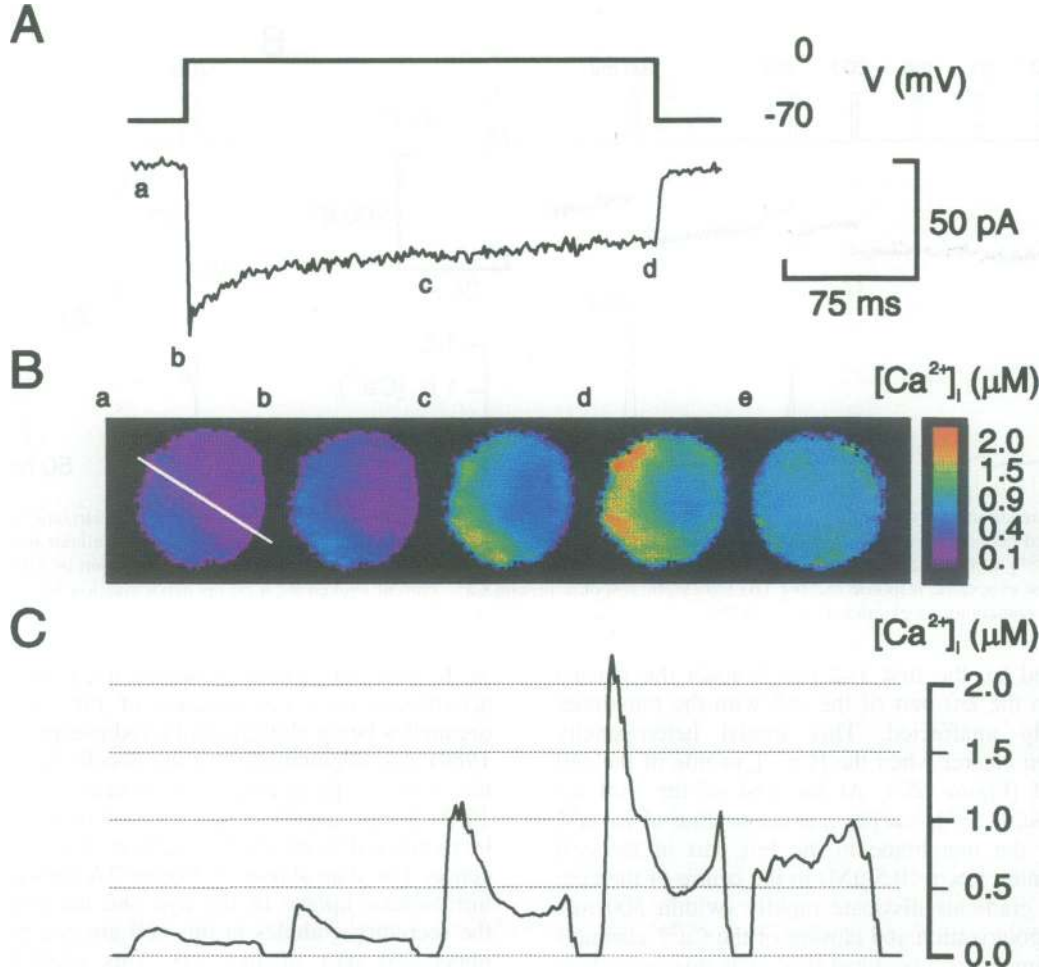

Fig. 2. Local Ca^{2+} gradients associated with exocytosis. (**A**) The Ca^{2+} current (lower) evoked by the 200 ms depolarization (top) from −70 to 0 mV. Same experiment as shown in Figure 1. (**B**) Spatial distribution of $[Ca^{2+}]_i$. The images were taken at the time points a–d indicated below the current trace in A. Image e was taken 300 ms after the end of the depolarization. Colours correspond to $[Ca^{2+}]_i$ as indicated by the colour bar (right). (**C**) $[Ca^{2+}]_i$ profiles taken along the white line indicated in B(a). Cell diameter ~10 μm.

estimate the number of secretory granules in the B-cells. In the cell displayed in Figure 3, the first depolarization produced a capacitance increase of 200 fF and a 1.8% decrease in total quinacrine fluorescence (Figure 3B). The capacitance increase resulting from the fusion of a single insulin-containing secretory granule with the plasma membrane has been estimated as 1.7 fF (Ämmälä *et al.*, 1993a), as expected for a granule with a diameter of 230 nm (Dean, 1973) and a specific membrane capacitance of 10 fF/μm^2. The observed increase in cell capacitance therefore corresponds to the simultaneous release of 120 secretory granules and the total number of granules in this particular cell can be calculated to be 6500 (120/0.018). A similar value (5900) was obtained when the responses to the train of depolarizations were analysed in the same way. The average number of granules per cell in 10 different cells was thus estimated as 11000 ± 1700. This value is in close agreement with the 13 000 derived by electron microscopy (Dean, 1973).

Voltage-dependent Ca^{2+} channels co-localize with the secretory granules

It is tempting to speculate that Ca^{2+} entry occurs in the region of the cell containing the highest density of secretory granules and that these areas represent 'hot spots' of secretion. This possibility is explored in Figure 4 which shows the whole-cell Ca^{2+} current evoked by a depolarization to 0 mV, the associated increase in $[Ca^{2+}]_i$ and the distribution of the secretory granules in the same cell. Clearly, the part of the cell containing the secretory granules is the same as that in which the increase in $[Ca^{2+}]_i$ is particularly pronounced. Similar results were obtained in all five cells exhibiting a polarized distribution of quinacrine.

The existence of such 'hot spots' of Ca^{2+} entry is reinforced by the data presented in Figure 5, which shows single Ca^{2+} channel currents recorded from cell-attached patches formed close to the regions of the cell containing either weak ('cold'; n = 8) or strong ('hot'; n = 5) quinacrine fluorescence. The patches on 'hot' regions contained on average 3.2 ± 0.4 active channels (as estimated by the maximum number of superimpositions) whereas the 'cold' regions contained only 0.9 ± 0.2 active channels (P<0.001). The ensemble currents averaged 0.01 ± 0.01 pA and 0.30 ± 0.08 pA in the 'cold' and 'hot' regions, respectively (P<0.01). Consistent with earlier reports, these channels are likely to be of the L-type as they were sensitive to dihydropyridines such as nifedipine and BAY K8644 (Rorsman and Trube, 1986; Rorsman *et al.*, 1988; Smith *et al.*, 1989) but unaffected

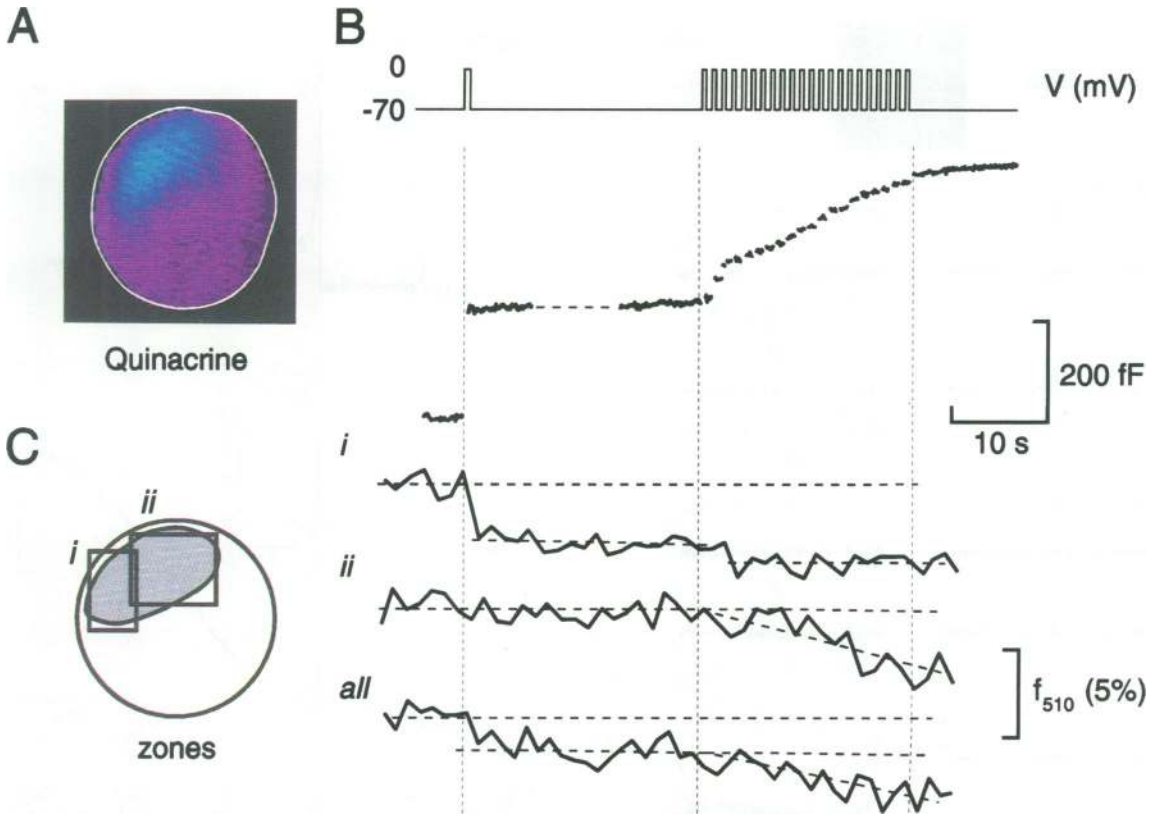

Fig. 3. Parallel recordings of secretion using microfluorimetry and capacitance measurements. (**A**) Fluorescence recording from a cell preloaded with quinacrine. Note uneven distribution of the dye within the cell. (**B**) Capacitance increases (middle) in response to a single 500 ms depolarization (top, left) and a train of 22 depolarizations (top, right) and the associated decrease in quinacrine fluorescence in the same cell (bottom trace). The loss of quinacrine fluorescence was analysed in three regions [i, ii and entire cell (='all')] as indicated in (**C**). The dashed horizontal lines indicate steady-state fluorescence intensities. The dashed vertical lines indicate either the onset or the end of a period of stimulation and have been inserted to facilitate temporal comparisons.

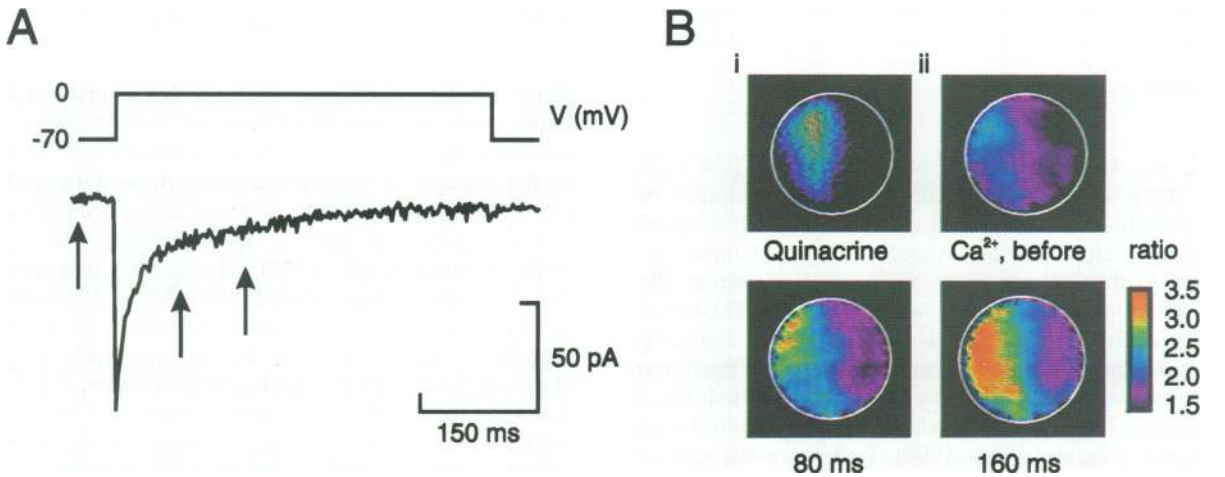

Fig. 4. Association between $[Ca^{2+}]_i$ increase and distribution of quinacrine fluorescence. (**A**) Voltage-clamp Ca^{2+} current (lower trace) elicited by a 500 ms depolarization from −70 mV to 0 mV. (**B**) (i) Localization of quinacrine fluorescence recorded in the cell subsequently used for the analysis of the $[Ca^{2+}]_i$ changes. (ii) Spatial distribution of $[Ca^{2+}]_i$ at the time points indicated by the arrows in (A).

by 1–2 μM ω-conotoxin GVIA, a blocker of N-type Ca^{2+} channels (Sher *et al.*, 1992; data not shown).

Estimation of the Ca^{2+}-dependence of exocytosis in the B-cell

The existence of specialized regions in the B-cell containing a high density of Ca^{2+} channels in close proximity to the secretory granules implies that the initiation of exocytosis requires higher $[Ca^{2+}]_i$ than is suggested by microfluorimetry, which only provides an average for the entire cell. To investigate further the $[Ca^{2+}]_i$ sensitivity of the secretory machinery in the B-cell we next produced uniform step increases in $[Ca^{2+}]_i$ by release of caged calcium from DM-nitrophen in cells voltage-clamped to −70 mV; i.e. too negative for Ca^{2+} channels to activate. Figure 6A shows the result of such an experiment. When

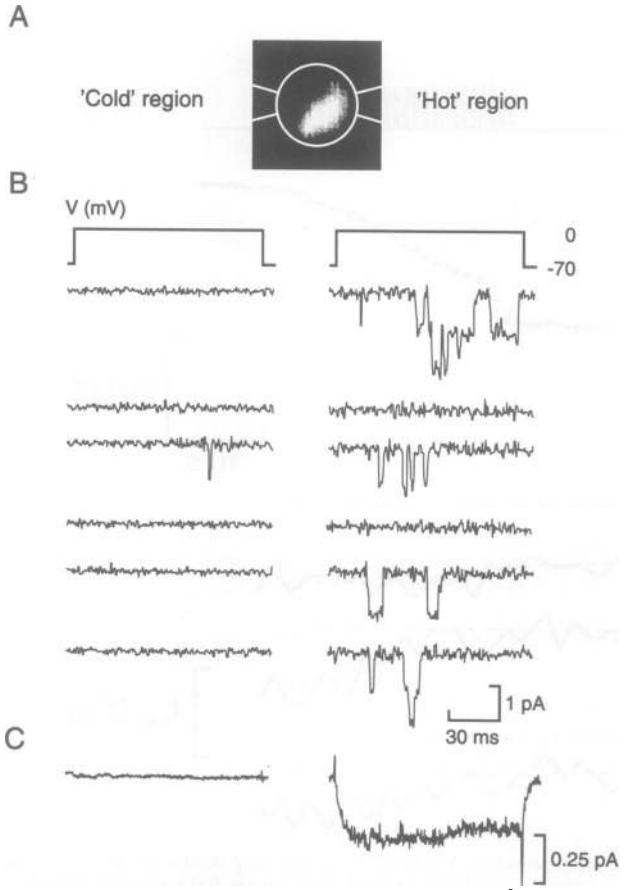

Fig. 5. Co-localization of secretory granules and L-type Ca^{2+} channels. (**A**) Distribution of quinacrine within a B-cell. (**B**) Ca^{2+} currents recorded simultaneously from two cell-attached patches formed at the cold (left) and hot (right) regions of the same cell as indicated schematically in (A) in response to membrane depolarizations from −70 mV to 0 mV. (**C**) Ensemble Ca^{2+} currents obtained by averaging single-channel activity in five (hot) or eight (cold) patches. Each experiment contained 128 sweeps and the mean currents shown were obtained by averaging the ensemble currents of the individual experiments.

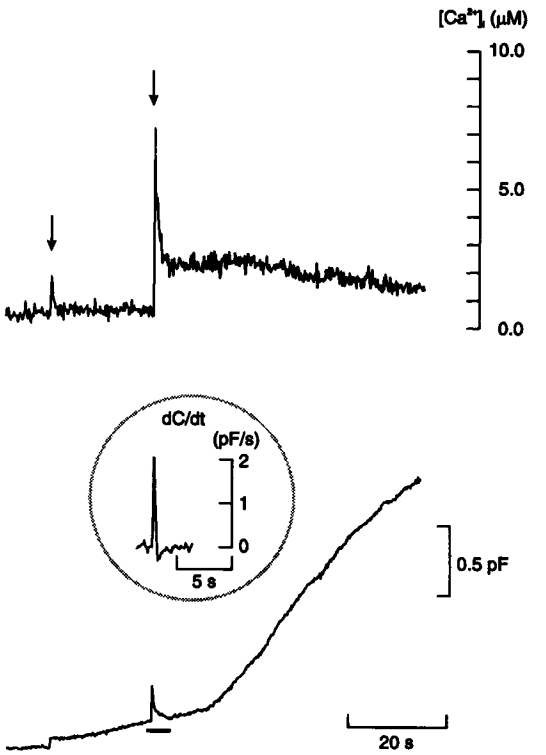

Fig. 6. $[Ca^{2+}]_i$ dependence of exocytosis. Effects on exocytosis evoked by increases in $[Ca^{2+}]_i$ (top) produced by photoliberation of 'caged' Ca^{2+} from DM-nitrophen. UV-light flashes were applied at the times indicated by the arrows. The first flash contained only 40% of the energy of the second flash. The cell was held at −70 mV throughout and the standard whole-cell configuration was used. (Inset) Rate of secretion (dC/dt) following the second flash during the 5 s marked by the horizontal line. The transitory nature of the $[Ca^{2+}]_i$ transient evoked by photolysis of DM-nitrophen we attribute to the binding of liberated Ca^{2+} to unaffected DM-nitrophen and/or wash-in of DM-nitrophen through the recording electrode.

$[Ca^{2+}]_i$ was elevated from a basal 0.3 to 1.8 μM (first flash), there was only a small capacitance increase of 75 fF. Within 1–2 s following the flash, $[Ca^{2+}]_i$ dropped to 0.6 μM, close to the average $[Ca^{2+}]_i$ obtained in response to the 200 ms pulse in Figure 1. However, the rate of secretion at this $[Ca^{2+}]_i$ was only 9 fF/s. The initial short-lived phase of exocytosis we explain by assuming that for a brief period during and following the flash, too short to be resolved by our recording system which has a resolution of 200 ms, $[Ca^{2+}]_i$ was higher than that reported by the dye (Kaplan *et al.*, 1990). Following the second flash, $[Ca^{2+}]_i$ transiently increased to >7 μM but subsequently stabilized at a concentration of ~2 μM. These changes in $[Ca^{2+}]_i$ produced an initial capacitance step of 260 fF which was then followed by a gradual decrease in membrane capacitance to the prestimulatory level. By analogy with previous observations in chromaffin and pituitary cells, we interpret the latter process as the endocytosis of secreted membranes (Thomas *et al.*, 1990; Neher and Zucker, 1993). Finally, 10 s after the flash, ongoing exocytosis at a rate of 49 fF/s is observed. Because $[Ca^{2+}]_i$ was not constant following the flash, it is difficult to determine whether the rapid and the slow phase of the capacitance increase have any functional implications. It seems likely however, that the initial short-lived and rapid phase of exocytosis (see inset) corresponds to the release of granules already docked beneath the membrane and that the slow phase reflects the release of granules mobilized from a reserve (Neher and Zucker, 1993; Thomas *et al.*, 1993). The 2 pF/s rate observed during the initial phase of the capacitance increase obtained in response to the second flash, when $[Ca^{2+}]_i$ was ~7 μM (Figure 6, inset), is close to the maximum response observed during a voltage-clamp depolarization (e.g. 1 pF/s; Ämmälä *et al.*, 1993a), suggesting that the $[Ca^{2+}]_i$ in the vicinity of the Ca^{2+} channels acting on the secretory granules may approach such high concentration.

Figure 7 shows the relation between maximal exocytotic rate (dC/dt) and $[Ca^{2+}]_i$. The different $[Ca^{2+}]_i$ levels were achieved by infusion of a buffered pipette (Ca/EGTA buffer) solution (n = 23), flash photolysis of caged Ca^{2+} (n = 20) or flash release of IP_3 from a caged inactive precursor (n = 12). The solid line is drawn to the best fit to equation (1),

$$\log_{10}[dC/dt] = \log_{10}[dC/dt_{max} * (1-1/1 + ([Ca^{2+}]_i/K_d)_n] \quad (1)$$

where dC/dt_{max} is the maximum rate of secretion, K_d the

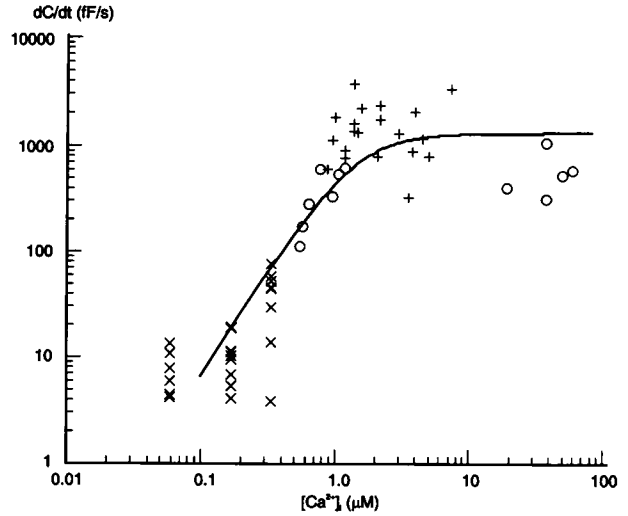

Fig. 7. Ca^{2+} dependence of secretion. The secretory rate (dC/dt) plotted as a function of $[Ca^{2+}]_i$. The various $[Ca^{2+}]_i$ levels were achieved by infusion of pipette solutions with $[Ca^{2+}]_i$ buffered to 60, 150 or 340 nM (x), flash photolysis of 'caged Ca^{2+}' (+) and a step increase in IP_3 (○) which produce a release of Ca^{2+} from intracellular stores (Ämmälä *et al.*, 1991). The solid line is drawn to the best fit of Equation 1.

Ca^{2+} concentration at which the rate of exocytosis is half-maximal and n the co-operativity coefficient. A least-squares fit of the above equation resulted in a K_d of 1.4 μM, a dC/dt_{max} of 1400 fF/s and a value of n of 2.0. A $[Ca^{2+}]_i$ of 4.2 μM is required to reach 90% of the maximal exocytotic rate.

Discussion

Using a combination of microfluorimetry, digital imaging, patch-clamp recordings and capacitance measurements of exocytosis we have explored the physical relationship between the voltage-dependent Ca^{2+} channels and the secretory granules in the insulin-secreting pancreatic B-cell and its significance for the initiation of secretion.

An important question naturally relates to the validity of the capacitance measurements we have used to monitor secretion. Several features, which are shared by insulin secretion, suggest that an increased cell capacitance can be equated to exocytosis of the insulin-containing granules. These include: (i) increases in cell capacitance are dependent on Ca^{2+} influx and are inhibited by Ca^{2+} channel blockers (Ämmälä *et al.*, 1993a); (ii) exocytotic responses can be modulated by activators and inhibitors of protein kinases and phosphatases (Ämmälä *et al.*, 1993b, 1994); and (iii) exocytosis as reflected by the capacitance measurements is highly dependent on temperature and is abolished at temperatures below 28°C (own unpublished data; Gillis and Misler, 1993). The present observation that an increased cell capacitance is correlated with a concomitant decrease of quinacrine fluorescence constitutes further evidence that a measurement of cell capacitance can be used to monitor secretion. Indeed, the number of secretory granules in a B-cell that can be derived by combining the quinacrine and capacitance data is close to that which has previously been obtained by electron microscopy.

A problem inherent to the use of Ca^{2+} chelators to visualize $[Ca^{2+}]_i$ gradients is that the indicator itself attenuates the $[Ca^{2+}]_i$ transients and thus interferes with cellular functions such as exocytosis (cf. Figure 1). We have addressed this problem by computer simulations using the model developed by Sala and Hernandez-Cruz (1990) for a spherical neuron. Figure 8 shows how $[Ca^{2+}]_i$ varies along the radius of the cell following a 50 ms depolarization in the absence (trace i) and presence (trace ii) of 50 μM fura-2. It is clear that the inclusion of fura-2 in the cytoplasm both reduces the amplitude of the $[Ca^{2+}]_i$ transient and limits the diffusion of Ca^{2+}. This is likely to constitute the explanation why a short pulse is insufficient to evoke secretion in the presence of the indicator. When the duration of the depolarization is increased to 200 ms, i.e. the first pulse to trigger exocytosis (Figure 1A), the $[Ca^{2+}]_i$ in the first 0.5–1 μm beneath the membrane approximates that elicited by the 50 ms depolarization in the absence of the dye and implies that this is the distance over which Ca^{2+} must diffuse in order to initiate secretion. This agrees favourably with the extent of the $[Ca^{2+}]_i$ transient actually observed experimentally in the imaging experiments (Figure 2) and we conclude therefore that Ca^{2+} needs to diffuse <1 μm from the Ca^{2+} channel(s) to activate the exocytotic machinery. The $[Ca^{2+}]_i$ in this region of the cell is, of course, much higher than the average $[Ca^{2+}]_i$ of the cell and may well approach the 7 μM measured in the 10% of the cells containing the highest Ca^{2+} concentrations. Indeed, this figure is close to the $[Ca^{2+}]_i$ at which the rate of exocytosis saturates (Figure 7). In this context it is of interest that electron microscopy has revealed that the first 0.2–0.4 μm of B-cell cytoplasm beneath the plasma membrane is almost devoid of secretory granules (see for example Pipeleers *et al.*, 1992). Thus, the ultrastructural and the imaging data both show that Ca^{2+} needs to diffuse some short distance to trigger secretion. Recent observations suggest that the latency between the onset of the depolarization and the initiation of secretion is 50–100 ms (own unpublished data). During this time Ca^{2+} may diffuse 1–2 μm in a buffered solution (estimated using the diffusion constant of Kasai and Petersen, 1994).

We demonstrate for the first time in pancreatic B-cells a functional co-localization of the insulin-containing secretory granules and L-type Ca^{2+} channels. This situation is clearly reminiscent of that in nerve terminals, where synaptic vesicles are situated in the immediate vicinity of Ca^{2+} channels (Robitaille *et al.*, 1990; Cohen *et al.*, 1991; Llinás *et al.*, 1992), or of that in exocrine gland cells where agonist stimulation leads to localized $[Ca^{2+}]_i$ changes in the secretory pole of the cell (Kasai *et al.*, 1993; Thorn *et al.*, 1993). Evidence has been provided that in the nerve terminals, a synaptic vesicle protein is required for Ca^{2+} channel function, and this has been suggested to account for the fact that increases in $[Ca^{2+}]_i$ co-localize with the distribution of synaptic vesicles (Mastrogiacomo *et al.*, 1994). We acknowledge that we cannot exclude that a similar mechanism is also operational in the B-cell. However, given the fact that the 'cold' regions do in fact contain L-type Ca^{2+} channels, albeit at a low density, we consider this possibility less plausible. Instead we favour the idea that the Ca^{2+} channels and secretory granules are

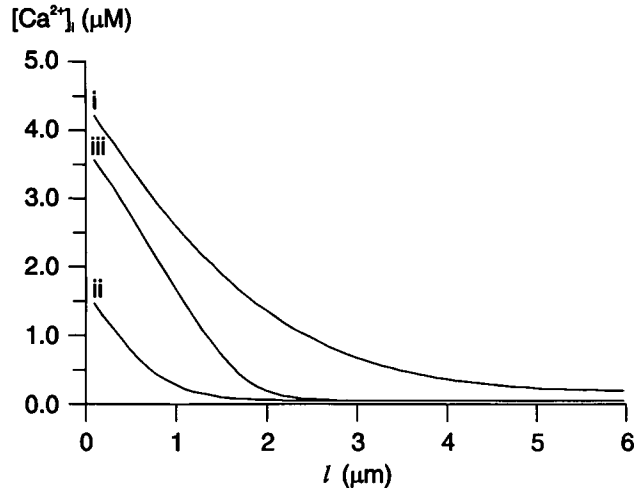

Fig. 8. Computer simulation of $[Ca^{2+}]_i$ within a B-cell at various distances from the plasma membrane. The radius of the cell was taken to be 6 μm (cf. Rorsman and Trube, 1986) and $[Ca^{2+}]_i$ calculated for a 50 ms voltage-clamp Ca^{2+} current with an amplitude of 100 pA (25×10^{-18} mol of Ca^{2+}) in the absence (i) or presence (ii) of 200 μM fura-2. Trace (iii) shows the calculated $[Ca^{2+}]_i$ distribution after a 200 ms Ca^{2+} current with an amplitude of 100 pA (100×10^{-18} mol) in the presence of 200 μM fura-2.

targeted, by some unestablished mechanism, to the same membrane region in the B-cell.

Regulation of exocytosis by a localized, rather than a global, increase in $[Ca^{2+}]_i$ is advantageous to the B-cell (Petersen *et al.*, 1994). First, it allows for a pronounced increase in $[Ca^{2+}]_i$ close to the regulatory site and thus, subsequent to the binding to low-affinity Ca^{2+} sensing proteins, produces large and rapid secretory responses. Secondly, as the increase in $[Ca^{2+}]_i$ is restricted to the small part of the cell where it mediates its second messenger function, the expenditure of metabolic energy to subsequently restore $[Ca^{2+}]_i$ to the resting concentration is minimized.

Materials and methods

Cells

NMRI mice were purchased from a commercial breeder (Alab, Sollentuna, Sweden). Mouse pancreatic islets were isolated by collagenase digestion and single cells prepared as previously described (Rorsman and Trube, 1986). Isolated cells were plated on glass coverslips (diameter 22 mm) and maintained in tissue culture for up to 2 days, but the experiments were usually carried out on the day of isolation or the first day of culture. The culture medium was RPMI 1640 containing 5 mM glucose and 10% (v/v) fetal calf serum and supplemented with 100 μg/ml streptomycin and 100 IU/ml penicillin. Coverslips were sealed over a circular hole (diameter 20 mm) in a standard petri dish (Corning) making a recording chamber in which the coverslip formed the base.

Electrophysiology

Whole-cell membrane currents were recorded using an EPC-7 patch-clamp amplifier (List electronic, Darmstadt, FRG). The zero-current potential of the pipette was adjusted with the pipette in the bath. The holding potential was −70 mV. The recordings were performed using either the perforated patch whole-cell configuration (Horn and Marty, 1988), which permits voltage-clamp recordings from functionally 'intact' cells, the cell-attached ('on-cell') mode or the standard whole-cell configuration (Hamill *et al.*, 1981).

To detect changes in membrane capacitance, which reflects exocytosis, a 20 mV r.m.s. 800 Hz sine wave was added to the holding potential (Joshi and Fernandez, 1988; Fidler Lim *et al.*, 1990) and 10 cycles were averaged for each data point. The resulting current was analysed at two orthogonal angles with a resolution of 100 ms per point. The phase angle was determined empirically for each experiments using the C_{slow} and G_{series} knobs on the amplifier, which are normally used to cancel the currents that result from the membrane capacitance of the cell and the series conductance of the electrode, respectively. Briefly, the G_{series} value was varied by 10 nS and the phase angle adjusted until no concomitant change of the capacitance trace was observed. The C_{slow} value was then decreased by 250 or 500 fF and the resulting change of the capacitance trace used to calibrate the exocytotic responses.

Single Ca^{2+} channel currents were recorded from cell-attached patches, close to regions of the cell with either high or low quinacrine fluorescence, using Ba^{2+} as the charge carrier. Only cells that were distinctly polarized with regard to the distribution of quinacrine were selected for this series of experiments. The single channel currents were filtered at 1 kHz (−3 dB) and digitized at 2 kHz. Leakage and capacitive transients were subtracted numerically using an average of sweeps not containing any channel activity.

Except for the recordings pertaining to Figures 4 and 5, which were conducted at room temperature, all experiments were performed at 31–33°C.

Solutions

The standard extracellular medium consisted of 118 mM NaCl, 20 mM TEA-Cl (to block voltage-gated K^+ currents), 5.6 mM KCl, 1.2 mM $MgCl_2$, 2.6 mM $CaCl_2$, 5 mM D-glucose, 5 mM HEPES (pH 7.4 with NaOH) and 2 μM forskolin (to enhance exocytosis; Ämmälä *et al.*, 1993b). In the perforated-patch recordings, the pipette solution consisted of 76 mM Cs_2SO_4, 10 mM NaCl, 10 mM KCl, 1 mM $MgCl_2$ and 5 mM HEPES (pH 7.35 with CsOH). Electrical contact was established by addition of the pore-forming antibiotic amphotericin B (Sigma, St Louis, USA) to the pipette solution. Briefly, a stock solution containing 6 mg of amphotericin dissolved in 100 μl DMSO was prepared and 20 μl of this stock solution were added to 5 ml of the pipette solution yielding a final concentration of 0.24 mg/ml. The tip of the pipette was filled with amphotericin-free solution and the pipette subsequently back-filled with amphotericin-containing solution. Perforation required a few min and the voltage-clamp regarded as satisfactory when the series conductance exceeded 40 nS.

The standard intracellular solution during conventional whole-cell recordings consisted of 110 mM potassium glutamate or caesium glutamate, 10 mM KCl, 10 mM NaCl, 3 mM MgATP, 0.01 mM EGTA and 5 mM HEPES (pH 7.15 using CsOH or KOH). To promote exocytosis, 0.1 mM Sp-cAMPS (BioLog, Bremen, Germany) was included in the pipette solution (Ämmälä *et al.*, 1993b).

For the single-channel recordings (Figure 5), the cells were immersed in a depolarizing high-K^+ solution containing 125 mM KCl, 30 mM KOH, 10 mM EGTA, 1 mM $MgCl_2$ and 5 mM HEPES (pH 7.15 using KOH) to ascertain full control over the membrane potential (Smith *et al.*, 1989). The pipette solution consisted of 120 mM $BaCl_2$ and 5 mM HEPES [pH 7.15 using $Ba(OH)_2$]. To increase Ca^{2+} channel activity, 2 μM of the dihydropyridine Ca^{2+} channel agonist BAY K8644 was added to the bath solution.

In one series of experiments (Figure 7), the free Ca^{2+} concentration of the pipette solution was clamped to concentrations between 0 and 0.34 μM by including 10 mM EGTA and 0–7 mM $CaCl_2$ (Augustine and Neher, 1992). In the experiments using caged Ca^{2+}, the pipettes contained a variant of the intracellular solution which consisted of 110 mM potassium glutamate, 10 mM KCl, 10 mM NaCl, 3 mM MgATP, 0.1 mM Sp-cAMPS, 25 mM HEPES (pH 7.15 with KOH) and 25 μM of the low-affinity Ca^{2+} indicator BTC (Molecular Probes, Eugene, OR, USA). Caged Ca^{2+} was added as either 8 mM DM-nitrophen (Calbiochem, San Diego, CA, USA)/ 2 mM Ca^{2+} or 1 mM caged EGTA (Molecular Probes)/1 mM Ca^{2+}.

$[Ca^{2+}]_i$ measurements

$[Ca^{2+}]_i$ was estimated by dual excitation spectrofluorimetry using, unless otherwise indicated, fura-2 as the Ca^{2+} indicator. Prior to the measurement the cells were loaded with the ester form of fura-2 (0.2 μM) for 20–25 min.

The measurements were made using an Axiovert 135 inverted microscope with a Plan-Neofluar 100×/1.30 objective (Carl Zeiss, Germany). The focal depth of this objective, according to the specifications of the manufacturer is <2 μm, and the observed fluorescent light originates principally from the focal plane as suggested by the fact that a patch pipette containing 0.1–0.2 mM of the indicator placed slightly out of focus (2–5 μm) contributed negligibly to the observed fluorescence from the focal plane. Fura-2 fluorescence (510 nm) was recorded at video

rate (25 ratio images/s) using a fluorescence imaging system (IonOptix Inc., Milton, MA., USA) consisting of an intensified video camera synchronized to the excitation light source (340/380 nm) and a computer interface. Image data were stored on video tape and played back, digitized and processed off-line by a computer. Ratio images are synchronized to patch-clamps recordings with an error margin of ±20 ms. The spatial resolution using this equipment is ~1 μm (Cheung *et al.*, 1989). Images shown represent the average of two consecutive samples taken 40 ms apart. The times given in Figures 2 and 4 indicate the midpoint of the 80 ms sampling period. The fura-2 fluorescence signal was calibrated from single cells by dialysing the cell interior with 100 μM fura-2 and Ca^{2+}-EGTA buffers (Molecular Probes) with free Ca^{2+} concentrations ranging between 0 and 39.8 μM (Ämmälä *et al.*, 1993a). These data were fitted to the equation of Grynkiewicz *et al.* (1985) and used to calculate $[Ca^{2+}]_i$.

When combining the $[Ca^{2+}]_i$-imaging with recordings of quinacrine fluorescence (Figure 3), $[Ca^{2+}]_i$ was monitored using fura red (Molecular Probes) as the indicator instead of fura-2 as the excitation and emission wavelengths of the latter indicator overlap those of quinacrine. In these experiments the cells were first loaded with quinacrine as described below and then with the ester form of fura red (0.2 μM) for 20 min. Excitation of fura red was effected at 440 and 490 nm and emitted light recorded at 660 nm. The fura red signal was not calibrated as there was a slight interference with quinacrine and the $[Ca^{2+}]_i$ levels are therefore expressed as fluorescence ratios rather than absolute concentrations. To ascertain that quinacrine did not interfere with the fura red $[Ca^{2+}]_i$ measurements, two cells were loaded with quinacrine after $[Ca^{2+}]_i$ had been recorded. Results similar to those shown in Figure 4 were obtained.

The large step increases in Ca^{2+} obtained upon photolysis of caged Ca^{2+} were monitored using the low-affinity Ca^{2+}-selective probe BTC (Molecular Probes). Excitation was effected at 405 and 490 nm and emitted light recorded at 525 nm. These excitation wavelengths do not produce photolysis of the caged compound. The BTC signal was calibrated by obtaining the minimum (before the first flash) and maximum (after complete photolysis of all caged Ca^{2+}) fluorescence ratios. The BTC fluorescence signal was then converted to $[Ca^{2+}]_i$ using the equation of Grynkiewicz *et al.* (1985) and a K_d of 7 μM (Iatridou *et al.*, 1994).

Quinacrine measurements

Cells were loaded overnight with quinacrine (Sigma) by adding 0.2 μM of the dye to the tissue culture medium. Excitation was effected at 340 nm and emitted light collected at 510 nm. The data points represent averages of 20 images and the interval between each data point is 1.5 s. When correlating the changes in cell capacitance to changes in the quinacrine fluorescence (Figure 3) the recordings were made using the standard whole-cell configuration as the observed exocytotic responses are generally larger in this recording mode than in intact cells.

Photolysis of caged Ca^{2+}

Caged Ca^{2+} (DM-nitrophen; Calbiochem or NP-caged EGTA; Molecular Probes) was released by UV-flashes from an XF-10 photolysis apparatus (HiTech Scientific, Salisbury, UK). The standard whole-cell configuration was used and the cell held at −70 mV to avoid interference by Ca^{2+} entering through plasma membrane Ca^{2+} channels.

Data analysis

Data are presented as mean values ± SEM and statistical significance was evaluated using Student's *t*-test.

Acknowledgements

Supported by the Juvenile Diabetes Foundation International, Novo-Nordisk A/S (Bagsvaerd, Denmark), the Swedish Medical Research Council, the Nordic Insulin Foundation Committee, the Swedish Diabetes Association, the Svenska Odd Fellow Ordens Humanitära Fond, the Magn. Bergvalls Stiftelse, the Swedish Society for Medicine and the Åke Wibergs Stiftelse.

References

Abrahamsson,H. and Gylfe,E. (1980) *Acta Physiol. Scand.*, **109**, 113–114.
Ämmälä,C., Larsson,O., Berggren,P.-O., Bokvist,K., Juntti-Berggren,L., Kindmark,H. and Rorsman,P. (1991) *Nature*, **353**, 849–852.
Ämmälä,C., Eliasson,L., Bokvist,K., Larsson,O., Ashcroft,F.M. and Rorsman,P. (1993a) *J. Physiol.*, **472**, 665–688.
Ämmälä,C., Ashcroft,F.M. and Rorsman,P. (1993b) *Nature*, **363**, 356–358.
Ämmälä,C., Eliasson,L., Bokvist,K., Berggren,P.-O., Honkanen,R.E., Sjöholm,Å. and Rorsman,P. (1994) *Proc. Natl Acad. Sci. USA*, **91**, 4343–4347.
Atwater,I., Ribalet,B. and Rojas,E. (1978) *J. Physiol.*, **278**, 117–139.
Augustine,G.J. and Neher,E. (1992) *J. Physiol.*, **450**, 247–271.
Bonner-Weir,S. (1988) *Diabetes*, **37**, 616–621.
Breckenridge,L.J. and Almers,W. (1987) *Proc. Natl Acad. Sci. USA*, **84**, 1945–1949.
Cheung,J.Y., Tillotson,D.L., Yelamarty,R.V. and Scaduto,R.C.Jr. (1989) *Am. J. Physiol.*, **256**, C1120–C1130.
Cohen,M.W., Jones,O.T. and Angelides,K.J. (1991) *J Neurosci.*, **11**, 1032–1039.
Dean,P.M. (1973) *Diabetologia*, **9**, 115–119.
Fidler Lim,N., Nowycky,M.C and Bookman,R.J. (1990) *Nature*, **344**, 449–451.
Gillis,K.D. and Misler,S. (1993) *Pflügers Arch.*, **424**, 195–197.
Grynkiewicz,G., Poenie,R.Y. and Tsien,R.Y. (1985) *J. Biol. Chem.*, **260**, 3440–3450.
Gylfe,E., Grapengiesser,E. and Hellman,B. (1991) *Cell Calcium*, **12**, 229–240.
Hamill,O.P., Marty,A., Neher,E., Sakmann,B. and Sigworth,F.J. (1981) *Pflügers Arch.*, **391**, 85–100.
Horn,R. and Marty,A. (1988) *J. Gen. Physiol.*, **92**, 145–159.
Iatridou,H., Foukaraki,E., Kuhn,M.A., Marcus,E.M., Haugland,R.P. and Katerinopoulus,H.E. (1994) *Cell Calcium*, **15**, 190–198.
Joshi,C. and Fernandez,J. (1988) *Biophys. J.*, **53**, 885–892.
Kaplan,J.H. (1990) *Annu. Rev. Physiol.*, **52**, 897–914.
Kasai,H. and Petersen,O.H. (1994) *Trends Neurosci.*, **17**, 95–101.
Kasai,H., Li,Y.X. and Miyashita,Y. (1993) *Cell*, **74**, 669–677.
Llinás,R., Sugimore,M. and Silver,R.B. (1992) *Science*, **256**, 677–679.
Lundquist,I., Ahrén,B., Håkansson,R. and Sundler,F. (1985) *Diabetologia*, **28**, 161–166.
Mastrogiacomo,A., Parsons,S.M., Zampighi,G.A., Jenden,D.J., Umbash,J.A. and Gundersen,C.B. (1994) *Science*, **263**, 981–982.
Neher,E. and Marty,A. (1982) *Proc. Natl Acad. Sci. USA*, **79**, 6712–6716.
Neher,E. and Zucker,R.S. (1993) *Neuron*, **10**, 21–30.
Petersen,O.H., Petersen,C.C.H. and Kasai,H. (1994) *Annu. Rev. Physiol.*, **56**, 297–319.
Pipeleers,D., Kiekens,R. and In't Veld,P. (1992) In Ashcroft,F.M. and Ashcroft,S.J.H. (eds), *Insulin: Molecular Biology to Pathology*. IRL Press, Oxford, pp. 5–31.
Pralong,W.F., Bartley,C. and Wollheim,C.B. (1990) *EMBO J.*, **9**, 53–60.
Prentki,M. and Matchinsky,F.M. (1987) *Physiol. Rev.*, **67**, 1185–1248.
Robitaille,R., Adler,E.M. and Charlton,M.P. (1990) *Neuron*, **5**, 773–779.
Rorsman,P. and Trube,G. (1986) *J. Physiol.*, **374**, 531–550.
Rorsman,P., Ashcroft,F.M. and Trube,G. (1988) *Pflügers Arch.*, **412**, 597–603.
Sala,F. and Hernandez-Cruz,A. (1990) *Biophys. J.*, **57**, 313–324.
Sher,E., Biancardi,E., Pollo,A., Carbone,E., Li,G., Wollheim,C. and Clementi,F. (1992) *Eur. J. Pharmacol.*, **216**, 407–414.
Smith,P.A., Rorsman,P. and Ashcroft,F.M. (1989) *Nature*, **342**, 550–553.
Theler,J.M., Mollard,P., Guérinau,N., Vacher,P., Pralong,W.F., Schlegel,W. and Wollheim,C.B. (1992) *J. Biol. Chem.*, **267**, 18110–18117
Thomas,P., Surprenant,A. and Almers,W. (1990) *Neuron*, **5**, 723–733.
Thomas,P., Wong,J.G., Lee,A.K. and Almers,W. (1993) *Neuron*, **11**, 93–104.
Thorn,P., Lawrie,A.M., Smith,P., Gallacher,D.V. and Petersen,O.H. (1993) *Cell*, **74**, 661–668.

Received on September 13, 1994; revised on October 19, 1994